Electron dynamics in chromium probed with 20-fs optical pulses

H. Hirori, T. Tachizaki, O. Matsuda, and O. B. Wright*
Department of Applied Physics, Faculty of Engineering, Hokkaido University, Sapporo 060-8628, Japan
(Received 17 March 2003; published 16 September 2003)

Electron excitation and relaxation in chromium are probed with 20-fs time resolution using an ultrafast optical technique. We obtain good fits to the data for the transient reflectivity and transmittivity changes in a thin film using a simple model of electron relaxation, suggesting the existence of an efficient electron-electron thermalization process on ultrashort-time scales. Quantitative analysis allows the extraction of thermo-optic coefficients and dielectric constant variations related to both the electron and the lattice temperatures.

DOI: 10.1103/PhysRevB.68.113102 PACS number(s): 78.47.+p, 78.20.Nv, 78.20.Ci

Nonequilibrium electron distributions can be excited in metals with an ultrashort light pulse.[1] The subsequent energy exchange between the electrons and the lattice is governed predominantly by the electron-phonon (e-p) scattering time, but is also affected by the electron-electron (e-e) scattering time. The noble metals, possessing simple band structures, have provided a fertile testing ground for theories of nonequilibrium electron relaxation and diffusion.[2–8] It is now possible to investigate the electron dynamics on time scales of the order of the e-e scattering time, typically 10–50 fs for excess electron energies ~1 eV. Although in the noble metals and in the alloy $CoPt_3$, where the e-p interaction is relatively weak, the evolution of such transient athermal electron distributions was investigated with ~20-fs time resolution,[7–9] in other transition metals no studies have been made on these time scales, to the best of our knowledge.

The group-VIB transition metals (Cr, Mo, W) are interesting because they have large values of the e-p coupling constant, resulting in short electron energy relaxation times ~200 fs compared to the noble metals (~1 ps).[10] Their band structure is complicated, there being a significant density of states due to *d* electrons in the region around the Fermi level.[11] Understanding the short-time electron dynamics in such metals with strong e-p coupling should become essential for applications in future ultrafast devices with ultrahigh switching speeds. The electron relaxation in thin films of chromium and tungsten under spatially homogeneous conditions was measured by Brorson *et al.* with optical pulses of duration 60 fs.[10] But only the reflectivity change was probed, thus preventing access to the transient dielectric constant. In this report we monitor both the reflectivity and transmittivity changes in a thin polycrystalline film of chromium with 20-fs optical pulses to elucidate the ultrafast dynamics of the electrons therein.

The film of Cr on a crown glass substrate is excited and probed from the front side with near Fourier-transform-limited optical pulses from a Ti:sapphire laser (Kapteyn-Murmane Labs) of central wavelength 790 nm, repetition rate 87 MHz, pulse duration $\tau_L = 20$ fs [full width at half maximum (FWHM) intensity], and spectral width ~50 nm (FWHM). A schematic diagram of the apparatus is shown in Fig. 1. Interband transitions of electrons within the photon energy (1.57 eV) of the Fermi surface (at $\varepsilon_F \approx 7$ eV) are primarily induced.[11] The optical pulse duration is controlled by two prisms. It is measured at the sample position by a noncollinear cross-correlation technique, through the temporary insertion of a 25-μm slab of beta barium borate that combines the cross-polarized pump and probe beams at 0° and 10° (*p*-polarized) incidence, respectively. At the sample the optical spot radius at $1/e$ intensity is $a \approx 9.5\ \mu$m, the typical incident pump pulse energy is $E = 0.75$ nJ (maximum incident fluence $E/\pi a^2 \approx 0.26\ \mathrm{mJ\,cm^{-2}}$), and the probe pulse energy is 0.007 nJ. The predicted electron temperature change (for a thermalized electron gas) is 220 K and that of the lattice is 8 K. The pump light is chopped mechanically at 2 kHz, and a synchronous signal proportional to the reflected or transmitted intensity variation of the probe light is fed to a lock-in amplifier. Multiple scanning with an optical delay line allows a resolution for relative intensity changes $\sim 5 \times 10^{-6}$ (with a total integration time of ~2 s per point with 280 points, using 60 scans).

The polycrystalline Cr sample of thickness $d_0 = 19$ nm is prepared on a crown glass substrate of thickness 1 mm at a pressure of 5×10^{-6} Torr by electron-beam deposition at 0.3 $\mathrm{nm\,s^{-1}}$.[12] The grain size was estimated by atomic force microscopy to be 100–200 nm. The thickness is measured by spectroscopic ellipsometry and confirmed with picosecond ultrasonics.[13] The refractive index of the film ($n + i\kappa = 3.65$

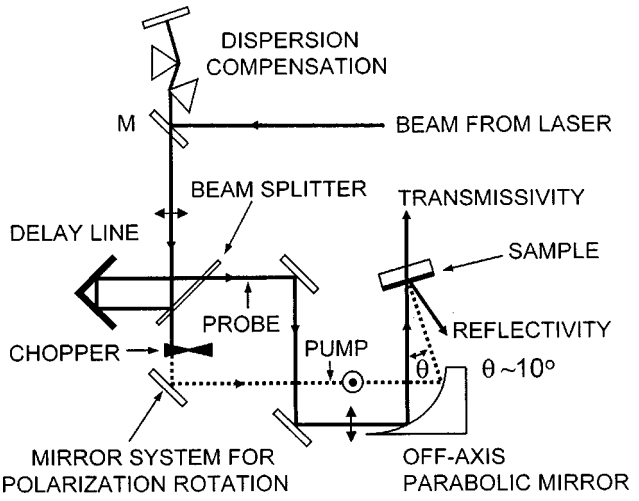

FIG. 1. Schematic diagram of the experimental setup. The beam exiting from the dispersion-compensation prisms passes below the mirror M. The first reflection from the beam splitter, a glass slide of thickness 1 mm, is used for the probe.

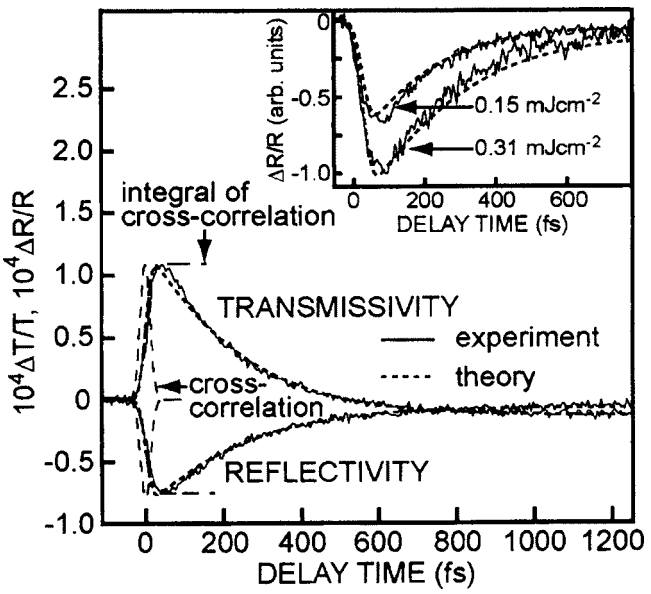

FIG. 2. Comparison of the relative reflectivity and transmissivity changes, $\Delta R/R$ and $\Delta T/T$, measured (solid curves) for a 19-nm Cr film with FWHM optical pulse duration $\tau_L = 20$ fs at 1.57 eV (790 nm), and calculated (dotted curves) using the two-temperature model. The pump fluence is 0.26 mJ cm^{-2}. Also shown are the pump-probe cross correlation (dashed curve) and its integral (dash-dotted curve). The inset shows a comparison of the relative reflectivity changes measured (solid curves) and fitted (dotted curves—fitted simultaneously with the same values for *a*, *b*, *c*, *d*, and *g* as above and appropriate lattice temperatures) for $\tau_L = 34$ fs using the two-temperature model for pump fluences 0.31 and 0.15 mJ cm^{-2}, respectively.

$+3.09i$) and substrate ($n_s = 1.52$) at 790 nm are also measured by ellipsometry. This value of κ corresponds to a 20-nm optical-absorption depth. The measured static reflection and transmission coefficients of the sample for the ultrashort optical pulses are, respectively, $R \approx 0.46$ and $T \approx 0.16$. These values are close to those ($R \approx 0.43$ and $T \approx 0.12$) expected from the measured $n + i\kappa$ for normally incident monochromatic light at 790 nm. We expect a nearly homogeneous (to within 10%) optical-absorption profile in the depth direction in the film. With the steady-state sample temperature in the probed region estimated at ≈470 K,[14] Cr is in its paramagnetic state. (Exposure to a temperature of this order during the experiment is not expected to significantly increase the native oxide layer thickness on the sample, of the order of a few nm in thickness, that should have a negligible effect on the present measurements.[15])

Figure 2(a) shows the experimental relative reflectivity and transmittivity changes (solid curves) as a function of delay time. The initial change in the signals is compared with the integral (dash-dotted curves) of the cross correlation (dashed curves) for the pump and probe optical pulses. The data follow closely behind this integral in the initial stages. The sign of ΔR (dependent on film thickness[16]) is opposite to that of ΔT. The simplest theoretical model that can account for this data reasonably well is the two-temperature model:[17] the electrons and the lattice are assumed to be described by separate temperatures T_e and T_l, coupled by the e-p interaction. In a one-dimensional approximation, valid since $a \gg d_0$,

$$C_e(T_e)\frac{\partial T_e}{\partial t} = -g(T_e - T_l) + S(z,t), \tag{1}$$

$$C_l\frac{\partial T_l}{\partial t} = g(T_e - T_l), \tag{2}$$

where z is the depth coordinate. The e-p coupling constant g and the lattice heat capacity C_l are assumed to be constant because of the relatively small transient change in lattice temperature (~10 K).[1,18] The electron heat capacity, about 35 times smaller than C_l (≈3.6 Jm^{-3}K^{-1} at 470 K), is given by $C_e(T_e) = \gamma T_e$ ($\gamma = 193$ Jm^{-3}K^{-2}).[19] The source term due to the optical pulse is taken as

$$S(t) = 2K\sqrt{\frac{\ln 2}{\pi}}\frac{E}{\pi a^2}\frac{(1-R-T)}{d_0\tau_L}\exp\left[-4\ln 2\left(\frac{t}{\tau_L}\right)^2\right],$$

where the factor $K = \frac{1}{2}$ here is calculated to account for the spot size of the probe beam. Because of the poor air and substrate thermal diffusivities, we assume no transport of heat (or electrons) across the film boundaries on our experimental time scales.

Neglecting the small modulation from the substrate on our time scales, the reflectance (r) and transmittance (τ) changes ($\ll 1$) for the present geometry can be calculated from the transient dielectric constant change $\Delta\varepsilon = \Delta(n + i\kappa)^2$ of the film by assuming monochromatic incident radiation and spatially homogeneous modulation:[20]

$$\frac{\delta r}{r} = \frac{ik_0\Delta\varepsilon}{2a_0b_0}\int_0^{d_0}(a_1e^{ik_1z} + b_1e^{-ik_1z})^2dz, \tag{3}$$

$$\frac{\delta\tau}{\tau} = \frac{ik_0\Delta\varepsilon}{2a_0}\int_0^{d_0}(a_1e^{ik_1z} + b_1e^{-ik_1z})(a_1'e^{ik_1z} + b_1'e^{-ik_1z})dz, \tag{4}$$

where k_0 and k_1 are wave numbers and a_0, b_0, a_1, b_1, a_1', and b_1' are constants,[21] for which 0 refers to air and 1 to the film. The measured relative reflectivity ($\Delta R/R$) and transmittivity ($\Delta T/T$) changes are related to Eqs. (3) and (4) by $\Delta R/R = 2\,\mathrm{Re}(\delta r/r)$, $\Delta T/T = 2\,\mathrm{Re}(\delta\tau/\tau)$ [since $R = |r|^2$ and $T = |t|^2$]. Here, $\Delta\varepsilon$ is assumed to be linearly related to the electron and lattice temperature changes for our range of fluences. Measurements and fits for ΔR at different pump fluences (with $\tau_L = 34$ fs—see Fig. 2 inset) confirm that this first-order approximation is reasonable:[22]

$$\Delta\varepsilon = \Delta\varepsilon_1 + i\Delta\varepsilon_2 = (a\Delta T_e + b\Delta T_l) + i(c\Delta T_e + d\Delta T_l), \tag{5}$$

where $a = \partial\varepsilon_1/\partial T_e$, $b = \partial\varepsilon_1/\partial T_l$, $c = \partial\varepsilon_2/\partial T_e$, and $d = \partial\varepsilon_2/\partial T_l$. We treat these thermo-optic coefficients and g as fitting parameters, substituting the numerical solution of the nonlinear Eqs. (1) and (2) obtained by the finite-difference technique into Eqs. (3)–(5).[23] By least-squares fitting using parameters *a*, *b*, *c*, *d*, and *g* common to the two data curves in

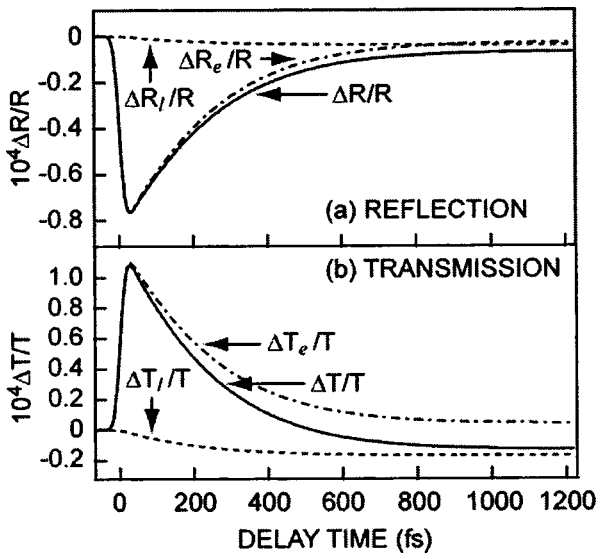

FIG. 3. (a) Calculated evolution of the relative reflectivity change $\Delta R/R$ (solid curve), and the separate electronic and lattice contributions to $\Delta R/R$: $\Delta R_e/R$ (dash-dotted curve) and $\Delta R_l/R$ (dashed curve), respectively. (b) Calculated evolution of the relative transmissivity $\Delta T/T$ (solid curve), and the electronic and lattice contributions to $\Delta T/T$: $\Delta T_e/T$ (dash-dotted curve) and $\Delta T_l/T$ (dashed curve), respectively. (In this figure only, ΔT_e and ΔT_l refer to changes in transmissivity rather than in temperature.)

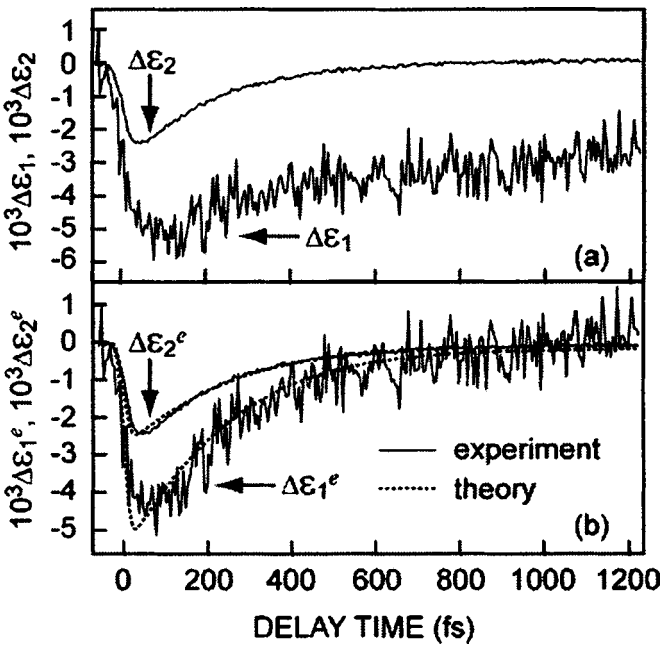

FIG. 4. (a) Measured transient changes of the real and imaginary parts $\Delta\varepsilon_1$ and $\Delta\varepsilon_2$ of the dielectric constant. (b) The extracted experimental electronic contributions to $\Delta\varepsilon$: $\Delta\varepsilon_1^e$ and $\Delta\varepsilon_2^e$ (solid curves). Theoretical curves (dotted) are also shown.

Fig. 2, and including a convolution with the probe pulse temporal profile, theoretical curves (dotted lines) are obtained that are very similar to experiment. This relative success of the two-temperature model may well extend to a wide range of optical wavelengths, considering the broad features in the joint density of states of the electrons in the VIB transition metals.[11,24]

The fitted value of $g=(470\pm30)\times10^{15}$ $\mathrm{Jm^{-3}\,K^{-1}}$ is in good agreement with (relatively temperature-insensitive[6]) literature values.[10,25] The thermo-optic coefficients obtained are $\partial\varepsilon_1/\partial T_e=-2.4\times10^{-5}$, $\partial\varepsilon_1/\partial T_l=-41\times10^{-5}$, $\partial\varepsilon_2/\partial T_e=-1.2\times10^{-5}$, and $\partial\varepsilon_2/\partial T_l=2.0\times10^{-5}$ in units of $\mathrm{K^{-1}}$. (The uncertainties are typically $\pm30\%$, owing mainly to the errors in the measurement of the pump fluence and in the multiparameter fitting.) These coefficients, sensitive to the band structure, are strong functions of wavelength.[11,26] Our low value for the ratio $(\partial\varepsilon_2/\partial T_l+\partial\varepsilon_2/\partial T_e)/(\partial\varepsilon_1/\partial T_l+\partial\varepsilon_1/\partial T_e)$ at 790 nm is consistent with that found in low-frequency thermomodulation measurements,[26] although the comparison is not exact because our experiments are done under conditions of approximately constant (zero) strain as opposed to constant (zero) stress.

The experimental $\Delta R/R$ and $\Delta T/T$ variations are difficult to interpret physically in terms of microscopic theories. The transient dielectric constant variation is more fundamental and is directly related to changes in the density of states governing the relevant electronic transitions. For our homogeneously excited thin film, the changes in ΔR and ΔT are linearly related to those in the dielectric constants:[4,5,8]

$$\Delta R/R=\alpha_1\Delta\varepsilon_1+\alpha_2\Delta\varepsilon_2, \tag{6}$$

$$\Delta T/T=\beta_1\Delta\varepsilon_1+\beta_2\Delta\varepsilon_2, \tag{7}$$

where the coefficients α_1, α_2, β_1, and β_2 can be obtained from Eqs. (3) and (4). Knowing the fitted $\Delta R/R$ and $\Delta T/T$ variations allows one to solve for the theoretical $\Delta\varepsilon_1$ and $\Delta\varepsilon_2$ variations, and in turn from Eqs. (3)–(5) for the theoretical electronic and lattice contributions to $\Delta R/R$ and $\Delta T/T$, as shown in Fig. 3 (based on values of α_1, α_2, β_1 and β_2 equal to 0.0025, 0.024, 0.0037 and -0.050, respectively). The lattice contribution for both the relative reflectivity [Fig. 3(a)] and transmissivity [Fig. 3(b)] changes tends to a constant value as the electron temperature relaxes. The contribution from the electron temperature change is dominant at short times in both cases.

Equations (6) and (7) also allow one to derive the experimental $\Delta\varepsilon_1$ and $\Delta\varepsilon_2$ variations (independent of any dynamical model), as shown in Fig. 4(a). Some salient points regarding these are as follows: (i) the temporal shape of $\Delta\varepsilon_2$ is similar to that of $\Delta R/R$ and $\Delta T/T$, and $\Delta\varepsilon_2$ is dominated by the electronic contribution; (ii) the temporal shape of $\Delta\varepsilon_1$ is different, and is strongly influenced by the lattice contribution; (iii) the noise level for $\Delta\varepsilon_1$ is significantly larger than that for $\Delta\varepsilon_2$. The results are a direct consequence of the signs and relative magnitudes of α_1, α_2, β_1, β_2 and of a, b, c, d. (iv) The magnitude of $\Delta\varepsilon_1$ is larger than that of $\Delta\varepsilon_2$, both quantities being negative. The sign of $\Delta\varepsilon_2$ indicates a decrease in absorption during the transient heating. The derived electronic contributions to the experimental dielectric constant variations, $\Delta\varepsilon_1^e$ and $\Delta\varepsilon_2^e$, are shown in Fig. 4(b). Comparison with the predictions of the two-temperature model (dashed curves) shows good agreement at times $t>100$ fs, suggesting that T_e is well defined at these

times and that the electron distribution is internally thermalized within ~100 fs by e-e scattering. By fitting the experimental $\Delta\varepsilon^e$ decays to the approximate function $\exp(-t/\tau^e_{1,2})$, the effective electron energy relaxation times τ^e_1 for $\Delta\varepsilon^e_1(t)$ and τ^e_2 for $\Delta\varepsilon^e_2(t)$ are found to be 230 ± 50 and 210 ± 20 fs, respectively. These values are longer than the value $\tau_e(T_e=T_l=470\ \mathrm{K})=C_e/g\approx190$ fs expected for the same initial lattice temperature in the limit of small ΔT_e. This increase in τ_e with increasing T_e is in agreement with rough estimates based on an approximate first-order solution to Eqs. (1) and (2) at constant T_l: $\tau_e\approx\tau_e(T_l)(1+T_e/T_l)/2$ (see Ref. 2). In a more sophisticated treatment the effect of the finite e-e relaxation time[27] and the band structure[11] should be taken into account. The variations $\Delta\varepsilon^e_1(t)$ and $\Delta\varepsilon^e_2(t)$ arise from a sum of all allowed electronic transitions at the probe wavelength originating in different regions of **k** space whose populations are perturbed by the pump optical pulse. These variations cannot be ascribed to a single interband transition in the complex band structure of Cr.[11,26] A more detailed analysis of the $\Delta\varepsilon$ variations is beyond the scope of this report.

In conclusion we have investigated the nonequilibrium dynamics of electron relaxation in chromium with 20-fs time resolution using an ultrafast optical technique. The two-temperature model produces good agreement with the experimental data, implying electron-electron thermalization within ~100 fs in this metal. This efficient thermalization and the short electron energy relaxation time in chromium bode well for future applications in ultrafast control of charge distributions and transport in transition metals.

We are grateful to Vitali Gusev and Hrvoje Petek for valuable discussions.

*Corresponding author. Electronic address: assp@kino-ap.eng.hokudai.ac.jp

[1] G. L. Eesley, Phys. Rev. B **33**, 2144 (1986).
[2] V. E. Gusev and O. B. Wright, Phys. Rev. B **57**, 2878 (1998).
[3] S. D. Brorson, J. G. Fujimoto, and E. P. Ippen, Phys. Rev. Lett. **26**, 1962 (1987).
[4] C. K. Sun, F. Vallee, L. H. Acioli, E. P. Ippen, and J. G. Fujimoto, Phys. Rev. B **50**, 15 337 (1994).
[5] S. Ogawa, H. Nagano, and H. Petek, Phys. Rev. B **55**, 10 869 (1997).
[6] R. H. M. Groeneveld and R. Sprik, Phys. Rev. B **51**, 11 433 (1995).
[7] N. Del Fatti, R. Bouffanais, F. Vallee, and C. Flytzanis, Phys. Rev. Lett. **81**, 922 (1998).
[8] N. Del Fatti, C. Voisin, M. Acherman, S. Tzortzakis, D. Christofilos, and F. Vallee, Phys. Rev. B **61**, 16 956 (2000).
[9] L. Guidoni, E. Beaurepaire, and J. Bigot, Phys. Rev. Lett. **89**, 017401 (2002).
[10] S. D. Brorson, A. Kazeroonian, J. S. Moodera, D. W. Face, T. K. Cheng, E. P. Ippen, M. S. Dresselhaus, and G. Dresselhaus, Phys. Rev. Lett. **18**, 2172 (1990).
[11] E. Colavita, A. Franciosi, C. Mariani, and R. Rosei, Phys. Rev. B **27**, 4684 (1983).
[12] Another sample of similar thickness made by the same technique at 5×10^{-7} Torr and 0.7 $\mathrm{nm\,s^{-1}}$ gave an identical reflectivity response, allowing us to conclude that the residual oxygen content of our film did not influence the results. See A. K. Kulkarni and L. C. Chang, Thin Solid Films **301**, 17 (1997).
[13] D. H. Hurley and O. B. Wright, Opt. Lett. **24**, 1305 (1999).
[14] This value, averaged over the probe beam profile, is estimated from a three-dimensional heat conduction model using the average absorbed pump power (12.4 mW), the Gaussian pump spot radius a, and the thermal conductivities of the substrate (1.4 $\mathrm{Wm^{-1}K^{-1}}$) and film (94 $\mathrm{Wm^{-1}K^{-1}}$).
[15] E. Idczak and E. Oleszkiewicz, Opt. Spetkrosk. **49**, 570 (1980) [Opt. Spectrosc. **49**, 309 (1980)].
[16] J. L. Hosteler, A. N. Smith, D. M. Czajkowsky, and P. M. Norris, Appl. Opt. **38**, 3614 (1999).
[17] S. I. Anisimov, B. L. Kapeliovich, and T. L. Perel'man, Zh. Eksp. Theor. Phys **66**, 776 (1974) [Sov. Phys. JETP **39**, 375 (1974)].
[18] T. Q. Qui and C. L. Tien, J. Heat Transfer **115**, 835 (1993).
[19] C. Kittel, *Introduction to Solid State Physics*, 7th ed. (Wiley, New York, 1996).
[20] O. Matsuda and O. B. Wright, J. Opt. Soc. Am. B **19**, 3028 (2002).
[21] Here k_0, k_1, and k_2 are the wave numbers in the air, film, and substrate, respectively, and $a_0=(k_0+k_1)(k_1+k_2)+(k_0-k_1)(k_1-k_2)e^{2ik_1d_0}$, $b_0=(k_0-k_1)(k_1+k_2)+(k_0+k_1)\times(k_1-k_2)e^{2ik_1d_0}$, $a_1=2k_0(k_1+k_2)$, $b_1=2k_0(k_1-k_0)e^{2ik_1d_0}$, $a_1'=(k_1-k_0)/2k_1$, and $b_1'=(k_0+k_1)/2k_1$.
[22] The measurements in the inset of Fig. 2 were also repeated in the range 0–150 fs at higher resolution to check the short-time response at different fluences. The characteristic slightly delayed response at short times compared to the two-temperature model was more clearly evident at both fluences.
[23] A. N. Smith, J. L. Hostetler, and P. M. Norris, Numer. Heat Transfer, Part A **35**, 859 (1999).
[24] W. B. Pickett and P. B. Allen, Phys. Rev. B **11**, 3599 (1975).
[25] T. Q. Qiu and C. L. Tien, Int. J. Heat Mass Transfer **37**, 2789 (1994).
[26] E. Colavita, A. Franciosi, D. W. Lynch, G. Paolucci, and R. Rosei, Phys. Rev. B **27**, 1653 (1983).
[27] V. P. Zhukov, F. Aryasetiawan, E. V. Chulkov, and P. M. Echenique, Phys. Rev. B **65**, 115116 (2002).